Acta Pharmaceutica Sinica B 2026;16(8):5297−5311

Chinese Pharmaceutical Association
Institute of Materia Medica, Chinese Academy of Medical Sciences

Acta Pharmaceutica Sinica B

www.elsevier.com/locate/apsb
www.sciencedirect.com

ORIGINAL ARTICLE

IFI30 reprograms glioblastoma-associated macrophage and induces immune evasion by MAFF/PTGS2 pathway

Sen Zhang[a,b,c,†], Wenlin Chen[d,†], Liwen Ren[a,b], Jie Yi[e], Xiangjin Zheng[f], Yihui Yang[a,b], Hong Yang[a,b], Guanhua Du[a,b], Wan Li[a,b], Yu Wang[d,*], Jinhua Wang[a,b,*]

[a]*The State Key Laboratory of Bioactive Substance and Function of Natural Medicines, Beijing 100050, China*
[b]*Beijing Key Laboratory of Innovative Drug Discovery and Polymorphic Druggability Research for Cerebrovascular Diseases, Institute of Materia Medica, Chinese Academy of Medical Science and Peking Union Medical College, Beijing 100050, China*
[c]*Air Force Medical Center, PLA, Air Force Medical University, Beijing 100142, China*
[d]*Department of Neurosurgery, Peking Union Medical College Hospital, Peking Union Medical College and Chinese Academy of Medical Sciences, Beijing 100730, China*
[e]*Department of Clinical Laboratory, Peking Union Medical College Hospital, Beijing 100730, China*
[f]*Department of Pharmacy, Medical Supplies Center, Chinese PLA General Hospital, Beijing 100853, China*

Received 28 April 2025; received in revised form 6 September 2025; accepted 6 January 2026

KEY WORDS

Glioblastoma multiforme;
Drug target;
IFI30;
Immune microenvironment;
Macrophage;
PTGS2;
MAFF;
CD8 T cell

Abstract In recent years, immunotherapy has shown obvious advantages in treating cancers. The close interaction between cancer cells and immune cells in the tumor microenvironment (TME) underlies the progression of glioblastoma multiforme (GBM). However, there are no effective immune-related targets against GBM. Here, *in silico* analyses and experimental data showed that Interferon Gamma Inducible Protein 30 (IFI30), modulated by histone modifications both H3K4me3 and H3K27ac, was up-regulated in GBM and had a potential role in the antitumor immune responses. *In vitro* and *in vivo* experiments further revealed that IFI30 modulated the infiltration of tumor-associated macrophages (TAMs) and reduced the proportion of $CD8^+$ T cells. Mechanistically, IFI30 induced PGE2 expression in GBM cells *via* the MAFF/PTGS2 pathway, and PGE2 bound to macrophage EP2/EP4, activating the

*Corresponding authors.
E-mail addresses: wjh@imm.ac.cn (Jinhua Wang), ywang@pumch.cn (Yu Wang).
[†]These authors contributed equally to this work.
Peer review under the responsibility of Chinese Pharmaceutical Association and Institute of Materia Medica, Chinese Academy of Medical Sciences.

https://doi.org/10.1016/j.apsb.2026.06.002
2211-3835 © 2026 The Authors. Published by Elsevier B.V. on behalf of Chinese Pharmaceutical Association and Institute of Materia Medica, Chinese Academy of Medical Sciences. This is an open access article under the CC BY-NC-ND license (http://creativecommons.org/licenses/by-nc-nd/4.0/).

downstream ERK1/2 and KLF4/STAT6 pathways, stimulating the infiltration of TAMs. Taken together, we characterized the role and mechanisms of IFI30 in the malignant progression of GBM by regulating TAMs, highlighting that IFI30 may benefit GBM patients as a therapeutic target.

© 2026 The Authors. Published by Elsevier B.V. on behalf of Chinese Pharmaceutical Association and Institute of Materia Medica, Chinese Academy of Medical Sciences. This is an open access article under the CC BY-NC-ND license (http://creativecommons.org/licenses/by-nc-nd/4.0/).

1. Introduction

Gliomas are currently the most common primary intracranial malignancies, with glioblastoma multiforme (GBM, grade IV) accounting for approximately 15% of all brain tumors[1]. Due to unclear pathogenesis, intricate biologic features, and limited therapeutic options, the prognosis of GBM patients is extremely poor. The recent success of immunotherapies, including immune checkpoint blockade (ICB) and chimeric antigen receptor (CAR)-T cell therapy in many cancers[2,3], has emphasized the promise and importance of immunotherapeutic strategies, but their consistent failures in GBM patients have been attributed to the "cold" immune microenvironment[4,5]. GBM is typically characterized by unresponsive and dysfunctional cytotoxic immune cells[6]. Although scientists have been attempting to activate the anti-tumor potential of the immune system[7,8], immunotherapies in GBM are still considered experimental[9,10], and further studies are needed to fully understand their efficacy and safety in GBM. To date, the Food and Drug Administration (FDA) has not approved any immunotherapies for GBM, it is warranted to explore differentiated immunotherapies for GBM in the future.

GBM is distinguished by low T cells and abundant tumor-associated macrophages (TAMs) infiltration, which account for 30%−50% of the entire tumor tissue[11]. Typically, classically activated macrophages (M1) engage in direct cytotoxicity or stimulate anti-tumor immune responses by enhancing the presentation of tumor-associated antigens[12,13]. Tumor signals, on the other hand, guide macrophages towards alternative activation (M2)[12−14], which directly promotes tumor progression by stimulating angiogenesis, preserving tumor cell stemness, and inducing drug resistance, and indirectly facilitates tumor immune evasion by mediating immune dysfunction within the tumor microenvironment (TME)[15,16]. M2-TAMs are known to enhance immunosuppression and contribute to the ineffectiveness of GBM immunotherapy[17], it is an intriguing possibility for re-educating M2-TAMs to function as anti-tumor effector cells. Studies have shown that complex crosstalk was established between GBM cells and TAMs[18]. Nevertheless, how tumors recruit TAMs to TME is still not completely understood, hampering the development of TAM-targeted strategies for cancer intervention.

Interferon Gamma Inducible Protein 30 (IFI30), also Gamma-Interferon-Inducible Lysosomal Thiol Reductase (GILT), participates in catalyzing the reduction of disulfide bonds[19] and the processing and presentation of disulfide-bond-containing antigens[20,21]. Importantly, recent studies have indicated that IFI30, which is abnormally expressed in many tumors, including GBM[22], diffuse large B-cell lymphoma[23], melanoma[24−26], and breast cancer[27,28], exerts an integral function in tumorigenesis, progression and immune monitoring, revealing the feasibility of targeting IFI30 to some extent. However, IFI30 may exhibit distinct roles in tumors with different immunogenicity. In GBM, elevated IFI30 is associated with a poorer survival rate[26,29,30], promoting tumor proliferation, migration, invasion and Epithelial-Mesenchymal Transition (EMT)[22,31−33], which may serve as an independent poor prognostic indicator in GBM. *In silico* studies have preliminarily found that the overexpression of IFI30 in GBM is associated with the immunosuppressive microenvironment[30,31]. Nevertheless, the exact mechanism by which IFI30 regulates the immune microenvironment of GBM remains a gap for further investigation.

In this study, we evaluated the expression and regulatory mechanisms of IFI30 in GBM, and revealed its intrinsic role in regulating immune microenvironment-mediated GBM progression. The results showed that the expression of IFI30 was elevated in GBM patients and regulated by histone modifications H3K4me3 and H3K27ac. The GBM orthotopic models demonstrated that the GBM-promoting effect of IFI30 may be mediated by regulating the anti-tumor immune response. *In vitro* and *in vivo* experiments further revealed that IFI30 modulated TAMs infiltration and reduced the proportion of $CD8^+$ T cells. Also, targeted depletion of TAMs in GBM abolished the role of IFI30 in tumor progression. Mechanistically, IFI30 facilitated PGE2 expression in GBM cells *via* the MAFF/PTGS2 pathway. PGE2 bound to macrophage EP2/EP4, activating the downstream ERK1/2 and KLF4/STAT6 pathways to regulate macrophage phenotype and infiltration. Overall, our findings reveal a crucial IFI30/MAFF/PTGS2 axis and provide a rationale for IFI30-based therapeutics of GBM targeting TAMs.

2. Materials and methods

2.1. Tumor specimens

The GBM tissue, serum, and corresponding normal samples were collected from patients with GBM in Peking Union Medical College Hospital. All relevant patients agreed and signed informed consent, and the experiment content had been reviewed and approved by the Ethics Committee of the Chinese Academy of Medical Sciences and Peking Union Medical College (No. K3358, Beijing, China).

2.2. Cell culture

The human GBM cell lines, U87 and U251, human acute monocytic leukemia cell line Thp-1, and human microglial cell line HMC3 were bought from Procell (Wuhan, China). The murine glioma cell lines GL261 were bought from BeNa (Pingdingshan, China).

All GBM cell lines and HMC3 were cultured in Dulbecco's modified Eagle's medium (DMEM) with 10% fetal bovine serum (FBS) (Procell, Wuhan, China). Thp-1 was cultured in RPMI-1640 supplemented with 10% FBS and pretreated with 100 ng/mL PMA

(MedChemExpress, NJ, USA) for 24 h to generate M0 macrophages.

2.3. Establishment of stable cell lines and transfection

For constructing GBM cell lines with stable overexpression/knockdown of IFI30, corresponding lentiviral vectors and control vectors were used to infect cells for 72 h, followed by selection with 2 μg/mL puromycin. For silencing of IFI30, MAFF and PTGS2, cells were transfected with specific siRNAs for 48 h using the Lipofectamine™ 3000 (Invitrogen, Grand Island, USA) following the manufacturer's instructions.

2.4. Enzyme-linked immunosorbent assay (ELISA)

The patient's serum and cell culture medium were centrifuged at $1000\times g$ for 20 min at 4 °C, and then the supernatant was analyzed with different ELISA kits (IFI30 ELISA Kit, DL-IFI30-Hu, DLDEVELOP, Wuxi, China; PGE2 ELISA Kit, 70-EK8103/2, MultiSciences, Hangzhou, China) according to the manufacturer's instructions.

2.5. Western blot

The total protein was extracted using RIPA lysis buffer supplemented with protease and phosphatase inhibitors, and the concentration was quantitatively determined by the BCA method. An equivalent quantity of proteins was separated by SDS-PAGE electrophoresis and transferred onto the polyvinylidenedifluoride (PVDF) membranes, which were subsequently blocked with 5% BSA and probed with diluted primary antibodies (Supporting Information Table S1) at 4 °C overnight. The membranes were at last incubated with secondary antibodies (Table S1). Immunoreactive bands were visualized by using chemiluminescence reagents in an ECL kit.

2.6. Chromatin immunoprecipitation-qPCR (ChIP-qPCR) assay

Cells were collected and washed once with PBS. The cells were cross-linked with 1% formaldehyde for 10 min, followed by quenching with 0.125 mol/L glycine for 5 min. Chromatin immunoprecipitation, including sample preparation, sonication, immunoprecipitation by specific antibodies, and purification, was conducted using the SimpleChIP® Enzymatic Chromatin IP Kit (9002, Cell Signaling Technology, MA, USA). Quantification of ChIP products was performed in a Bio-Rad detection system. Primers used in ChIP-qPCR are listed in Supporting Information Table S2.

2.7. In vivo GBM models

2.7.1. Animals

8-week-old NOD-SCID and BALB/c-nude immunodeficient mice (female) and C57BL/6 mice (female) (GemPharmatech, Nanjing, China) were employed in this study. All mice were raised in individual cages under 12 h/day light at 23 ± 2 °C with unrestricted access to food and water. The study was conducted under the Guide for the Care and Use of Laboratory Animals (NIH) and approved by the Animal Ethics Committee of Peking Union Medical College and Chinese Academy of Medical Sciences (No. 00004002, Beijing, China).

2.7.2. GBM orthotopic model

Harvested GL261-Ctrl and GL261-IFI30^{OE} cells were resuspended in PBS (4×10^3 cells/μL). NOD-SCID mice, BALB/c-nude mice and C57BL/6 mice were anesthetized with sodium pentobarbital (60 mg/kg), and a tiny hole was drilled through their skull (3 mm to the right and 0.5 mm anterior to the bregma). The GL261-NC/GL261-IFI30^{OE} orthotopic model was constructed by slowly injecting an aliquot of 5 μL cells into the striatum (3.3 mm to the depth) at a rate of 1 μL/min. Mice were administered 10 mg/kg celecoxib (Solarbio, Beijing, China) on alternate days for 21 consecutive days. At the end of the experiment, an MRI was performed to measure the tumor volume, and the brains were stored for subsequent analysis.

2.7.3. In situ TAM depletion assay

The GBM orthotopic model was established following the above animal experiment protocol. Briefly, GL261-Ctrl/GL261-IFI30^{OE} cells were injected into the striatum of C57BL/6 mice. A metal cannula was then implanted at the identical site and secured to the skull with dental cement. Clodronate liposome was administered to deplete macrophages in the GBM. Specifically, an injection tube was inserted into the metal cannula, and 1.5 μL of either control liposome or clodronate liposome (Clod, Yeasen, Shanghai, China) was delivered into the striatum at a rate of 1 μL/min every 3 days. On Day 21, the cannula was removed, and the tumor volume was scanned by MRI.

2.8. Immunohistochemistry (IHC) and immunofluorescence (IF)

Immunohistochemistry (IHC) and immunofluorescence (IF) were carried out on 10 μm frozen sections. Sections were incubated with the specific primary antibody (Table S1) at 4 °C overnight and incubated with the corresponding secondary/fluorescent secondary antibody (Table S1) for 2 h at room temperature (RT). Then, the immunohistochemical sections were detected with DAB and counterstained with hematoxylin. For immunofluorescence, the cell nuclei were stained with DAPI.

After the designed treatment, the cells were fixed with 4% paraformaldehyde−PBS, permeabilized and blocked with Triton X-100 (0.1%)−BSA (3%). Primary antibodies at the recommended dilutions (Table S1) were then used to stain cells at 4 °C overnight. After intensive washing, cells were labeled by secondary antibodies (Table S1) together with DAPI/Hoechst for 2 h. Images were visualized using fluorescence microscopy.

2.9. Flow cytometry analysis

Tumors were isolated and clipped into 1−3 mm pieces in serum-free medium containing collagenase-IV and DNase-I, which were digested for 1 h at 37 °C and subsequently filtered with a 70 μm filter to obtain the single-cell suspension. Antibodies (Supporting Information Table S3) were diluted for staining following the instructions. Flow cytometry was performed using Urit BF730 (URIT, Guangxi, China) and quantified by FlowJo V10 (FlowJo, OR, USA).

Single-cell suspensions of Thp1 and HMC3 were collected and then incubated with antibodies (Table S3) at 4 °C for 30 min. Following two washes, the stained cells were resuspended in 200 μL PBS, analyzed on a FACS Calibur flow cytometer (BD Biosciences, NJ, USA), and quantified using FlowJo V10 (FlowJo, OR, USA).

2.10. Reverse transcriptase quantitative real-time PCR (RT-qPCR)

Total RNA was extracted by RNAeasy™ Animal RNA Isolation Kit with Spin Column (Beyotime, Shanghai, China) following the instructions. Then, reverse transcription was carried out using HiFiScript gDNA Removal RT MasterMix (CWBIO, Taizhou, China). The expression abundance of mRNA was evaluated using RT-qPCR on a CFX thermal cycler (Bio-Rad, CA, USA). Primers used in RT-qPCR are listed in Supporting Information Table S4.

2.11. RNA sequencing and functional enrichment analyses

U87-NC and U87-IFI30 cells were collected and lysed with TRIzol reagent (Invitrogen, Carlsbad, USA) and sent to NOVOGENE (Beijing, China) for next-generation sequencing. The total RNA was qualified by Agilent 2100 Bioanalyzer. NEB libraries were generated, qualified, pooled, and sequenced using the Illumina NovaSeq 6000 sequencing platform (Illumina Inc., CA, USA) according to the instructions. Gene Ontology (GO) enrichment analyses of differentially expressed genes (DEGs) were performed by the Metascape website (https://metascape.org/gp/index.html). For Gene Set Enrichment Analysis (GSEA), all gene sets were acquired from the Wikipathways Database (wikipathways.org/).

2.12. Statistical analysis

Results are presented as mean ± standard error of mean (SEM). Two-tailed unpaired Student's *t*-test or one-way ANOVA with Dunnett's method was applied to analyze the statistical significance. A P value less than 0.05 was considered significant.

3. Results

3.1. IFI30 is highly expressed in GBM through histone modification and is associated with poor prognosis

To estimate the expression of IFI30 in GBM and investigate if it correlates with the progression of GBM, *in silico* assays were conducted using the GEPIA (http://gepia.cancer-pku.cn/), UALCAN (https://ualcan.path.uab.edu/), Oncomine (www.oncomine.org) and CGGA (http://www.cgga.org.cn/) databases. The results suggested that *IFI30* was highly expressed in various cancers including GBM (Fig. 1A). Compared with oligodendrocytoma and astrocytoma, the expression of *IFI30* in high-grade glioma, especially GBM, was the highest (Fig. 1B), which was closely associated with the poor prognosis of GBM patients. Survival analysis further supported that GBM patients with high expression of IFI30 had a low survival rate (Fig. 1C). Therefore, we hypothesized that IFI30 might contribute to the malignant progression of GBM. Subsequently, we characterized the expression level and prognostic value of IFI30 in patients with GBM. The results of Western blot and IHC showed that IFI30 was highly expressed in tumor tissues of GBM patients (Fig. 1D, E, and G). Meanwhile, the ELISA assay also showed elevated IFI30 in the serum of GBM patients (Fig. 1H), suggesting that IFI30 may serve as a feasible biomarker for the diagnosis of GBM.

Epigenetic modification refers to stable and heritable changes in gene expression and cell function without altering the DNA sequence[34], including histone modifications. To investigate the regulatory mechanism behind the aberrant expression of IFI30 in GBM, ChIP-seq data from the UCSC Human Genome Database (https://genome.ucsc.edu/) were utilized to identify probable histone modifications in the promoter of IFI30 and examine the associations with GBM. The results revealed that the transcriptional activation marks H3K4me3 and H3K27ac were enriched in the promoter of *IFI30* across several cell lines and GBM-associated samples (Supporting Information Fig. S1A−S1D). ChIP-qPCR also verified that H3K4me3 and H3K27ac were more fold-enriched in the *IFI30* promoter of U251 cells relative to U87 cells (Fig. 1I and J). Moreover, the inducers of H3K4me3 (KDM5-C70, PBIT) and H3K27ac (TSA) modification increased the expression of IFI30 in GBM cell lines (Fig. 1K and L). Analysis of the proteomic data in the UALCAN database revealed the up-regulation of histone methyltransferases and acetyltransferases in GBM, consistent with IFI30 (Fig. S1E and S1F). In addition, up-regulation of H3K4me3 and H3K27ac was also observed in the GBM tissues (Fig. 1D and E, and Fig. S1G), and was positively correlated with IFI30 expression (Fig. 1F).

Taken together, these results indicate that the expression of IFI30, regulated by the histone modification H3K4me3/H3K27ac, is up-regulated in GBM, which is closely associated with the degree of malignancy and poor prognosis of GBM patients.

3.2. IFI30 is involved in immunosuppressive pathway for GBM progression

RNA-Seq was used to reveal the mechanism by which IFI30 facilitates the progression of GBM. A total of 323 down-regulated genes and 256 up-regulated genes were detected in U87-IFI30 cells (Fig. 2A). GO enrichment analysis found that IFI30 was associated with immune response, cytokine production, etc (Fig. 2B). GSEA analysis also suggested the up-regulation of several tumor immune escape-related gene sets (Supporting Information Fig. S2A). To elucidate the relationship between IFI30 and tumor immunity, bioinformatics analysis was carried out to estimate the immune infiltration landscape. Surprisingly, a strong and positive correlation was observed between IFI30 and ImmuneScore in the TCGA dataset across various grades of glioma (Fig. S2B). And, IFI30 was also found to be associated with immunosuppressive factors of tumor cells (Fig. 2C). Analysis of immune cell infiltration further suggested that tumor tissues with higher IFI30 expression were accompanied with higher M2-macrophages, but not consistently with B-cells, neutrophils and dendritic cells (Fig. 2D, Fig. S2C and S2D). Additionally, correlation analyses strengthened this finding, with IFI30 expression found to be positively associated with M2-macrophage markers (CD206, CD163, IL10) (Fig. S2E) in TCGA−GBM datasets. Infiltrating TAMs are the critical components of the tumor-promoting microenvironment, with M2-TAMs being an important contributor to the development of GBM (Fig. S2F). GBM patients with a high percentage of M2-TAMs had a low survival rate (Fig. S2G). Interestingly, we also found that IFI30 was negatively correlated with $CD8^+$ T cell infiltration (Fig. S2C) and associated with factors of exhausted cytotoxic T-cells (Fig. S2H). These findings suggest that IFI30 participates in GBM immunosuppression.

To explore whether IFI30 is involved in the regulation of the tumor immune, GL261-Ctrl and GL261-$IFI30^{OE}$ cells were used to generate orthotopic tumors in immunodeficient or immunocompetent mice. It was found that in immunocompetent C57 mice, overexpression of IFI30 promoted GL261 tumor growth, with a tumor proliferation rate of approximately 337.7%, which was only about 117.8% and 225.1% in NOD/SCID mice and BALB/c-nude mice (Fig. 2E−I), indicating a potential role of

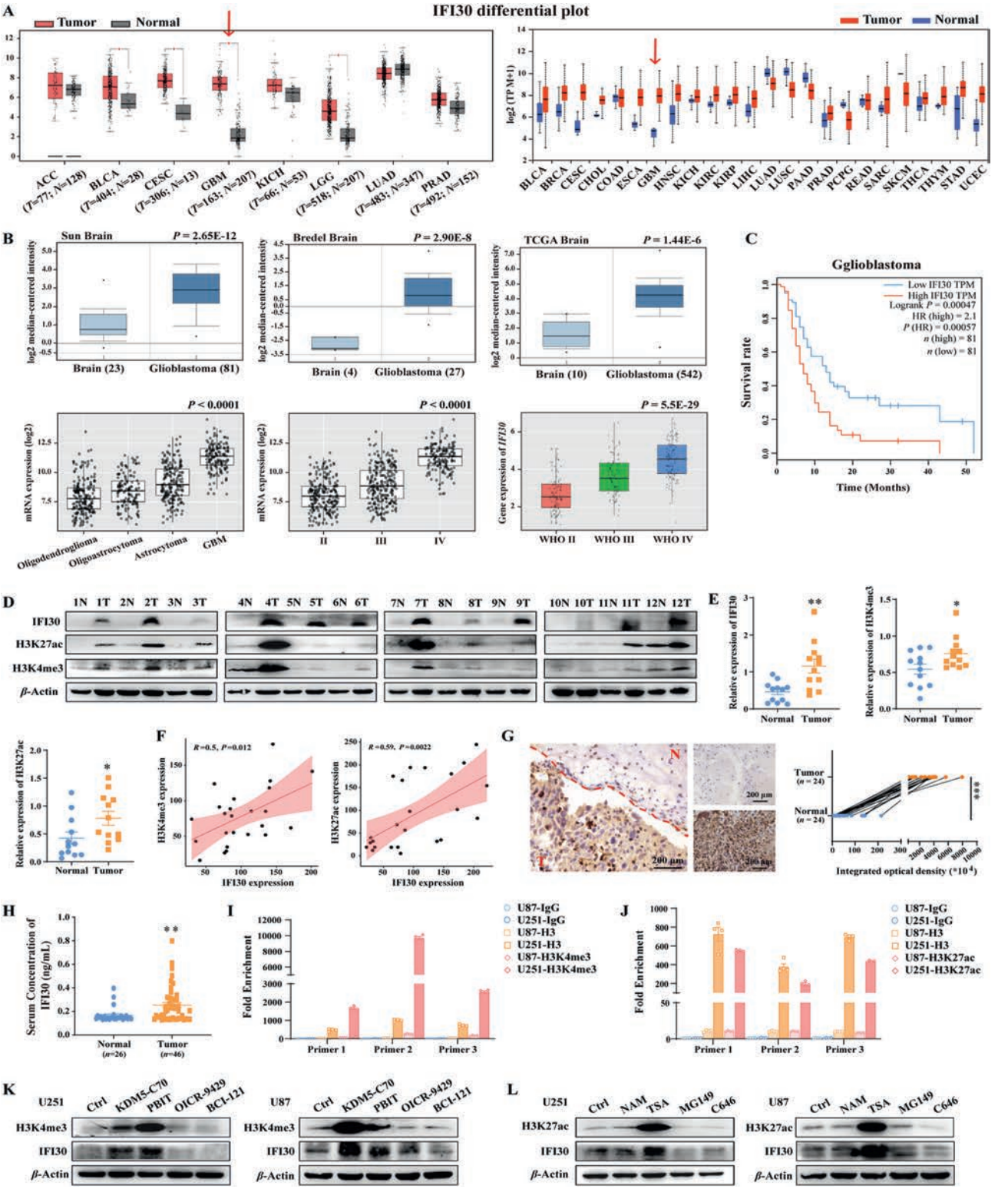

Figure 1 IFI30 is highly expressed in GBM through histone modification and is associated with poor prognosis. (A) Expression of *IFI30* was higher in GBM than in normal tissues. (B) *IFI30* was highly expressed in high-grade glioma, especially GBM. (C) Survival rate of GBM patients was analyzed on the website (http://gepia.cancer-pku.cn/). (D, E) IFI30, H3K4me3 and H3K27ac were highly expressed in tumor tissues (T) than adjacent normal tissues (N) of GBM patients. (F) The expression of IFI30 was positively correlated with that of H3K4me3 and H3K27ac in patients with GBM. (G) Representative images of IFI30 in normal tissues and GBM tissues (Scale bar = 200 μm). (H) The ELISA assay revealed an elevated level of IFI30 in the serum of GBM patients. (I, J) ChIP-qPCR analysis showed that H3K4me3 and H3K27ac were highly enriched in the promoter of *IFI30* in U251 cells relative to U87 cells. (K, L) Results from Western blot showed that KDM5-C70, PBIT and TSA induced the expression of H3K4me3, H3K27ac and IFI30 in U251 and U87 cells. Data are mean ± SEM of at least triplicate experiments. $^{**}P < 0.01$, $^{*}P < 0.05$.

IFI30 in regulating the antitumor immune responses. The effects of IFI30 on the GBM immune microenvironment were further detected by flow cytometry and immunofluorescence. It was observed that the infiltration of TAMs (Fig. 2J and M), especially M2-TAMs (Fig. 2K−M), was enhanced in IFI30-overexpressed tumor tissues. Consistently, overexpression of IFI30 also suppressed the infiltration of $CD8^+$ T cells (Fig. 2N and O) and reduced the percentage of interferon-γ^+ (IFNγ) $CD8^+$ T cells in the TME (Fig. 2P). Nevertheless, IFI30 did not affect the abundance and function of $CD4^+$ T cells (Fig. S2I and S2K). In summary, IFI30 induces the infiltration of TAMs and reduces the proportion of $CD8^+$ T cells in GBM tissues.

3.3. IFI30 induces PTGS2 expression in GBM cells to coordinate macrophages

To further validate the effects of IFI30 on TAMs in the GBM microenvironment, microglia/macrophages were co-cultured with the conditioned medium of IFI30-overexpressing or knockdown GBM cell lines, and the changes in their migratory and polarization state were promptly detected. Overexpression of IFI30 in U87 cells (Supporting Information Fig. S3A and S3B) altered macrophage morphology (Fig. 3A), promoted macrophage migration (Fig. 3B) and increased the expression of M2 markers (*CD163*, *CD206*, *IL10*, and *Arg 1*, Fig. 3C and D). Conversely, knockdown of IFI30 in U251 cells (Fig. S3C and S3D) inhibited macrophage migration (Fig. 3B) and polarization (Fig. 3E and F).

To delve into the mechanism by which IFI30 modulates TAMs in the GBM microenvironment, we screened GO terms in RNA-seq related to inflammation, leukocyte migration, cytokine production, etc., and identified tumor immune-related genes regulated by IFI30 (Fig. 3G). RT-qPCR assay showed that the mRNA levels of *CXCL8*, *CXCL3*, *CXCL2*, *PTGS2*, *IL6*, *TNF* and *IL1A* were increased in U87-IFI30 cells. Among them, prostaglandin-endoperoxide synthase 2 (PTGS2, COX2) showed one of the most notable changes (Fig. 3H) and was also the core target of the PPI network (Fig. S3E). The inducible enzyme PTGS2 functions as a crucial inflammatory marker by converting arachidonic acid to PGE2, and has been shown to promote the progression of tumors by stimulating cell division, inhibiting apoptosis, spurring neovascularization, and facilitating immune escape. Exogenous addition of PGE2 dramatically promoted the migration and M2-polarization of macrophage (Fig. S3F−S3H). To verify the regulatory role of IFI30 on PTGS2 expression, we initially examined whether PTGS2 was also highly expressed in GBM patients. Both Western blot assay and GEPIA database analysis confirmed that PTGS2 was elevated in tumor tissues of GBM patients compared with adjacent tissues (Fig. 3I and Fig. S3I). Moreover, the correlation analysis of TCGA revealed a positive association between *IFI30* and *PTGS2* (Fig. S3J). The results from RT-qPCR, Western blot and IF confirmed that both mRNA and protein expression of PTGS2 were regulated by IFI30 (Fig. 3H−J, K, and Fig. S3K). Consistently, in the GBM orthotopic model, mice in the $IFI30^{OE}$ group exhibited higher PTGS2 levels (Fig. S3L). On the other hand, results from ELISA showed that IFI30 endogenously drove the expression of PGE2 in GBM cells (Fig. 3J and K), suggesting that PTGS2 may be a downstream target of IFI30. Furthermore, we interrogated whether PTGS2 mediates the regulatory effect of IFI30 on macrophages. Knockdown of PTGS2 in U251 cells was found to inhibit the expression of PGE2 (Fig. 3L), leading to reduced macrophage migration (Fig. 3M). Crucially, silencing of PTGS2 suppressed IFI30-induced macrophage migration and polarization (Fig. 3N−Q). On the other hand, PTGS2 overexpression also reversed the IFI30-knockout-induced inhibition of macrophage migration and polarization (Fig. S3M and S3N). Collectively, the above results suggest that PTGS2 is responsible for the recruitment and polarization of macrophages induced by IFI30.

3.4. IFI30 enhances PTGS2 expression through the transcription factor MAFF

To investigate how IFI30 promotes PTGS2 expression in GBM cells, a Co-IP assay was applied and no direct interaction was found between IFI30 and PTGS2 (Fig. 4A). Further, we examined several transcription factors to ascertain whether they were involved in the regulation of PTGS2 expression by IFI30. The PROMO website and UCSC Human Genome Database were used to identify multiple transcription factors potentially implicated in PTGS2 regulation (Supporting Information Fig. S4A and S4B). By screening the transcriptomic data, *NR1D1*, *MAFF*, *TFAP2A*, and *ATF3* were up-regulated in U87-IFI30 cells and were identified as the transcription factors most likely mediating IFI30 function (Fig. 4B). The *in silico* analysis of TCGA data verified that only *MAFF* and *ATF3* exhibited the positive correlation with both *IFI30* and *PTGS2* (Fig. 4C). The levels of NR1D1, MAFF, TFAP2A, and ATF3 were examined by RT-qPCR and Western blot, and the results showed that IFI30 dramatically enhanced the mRNA and protein expression of MAFF (Fig. 4D−F). In addition, MAFF regulated the expression of PTGS2 (Fig. 4G), illustrating that MAFF mediated the regulatory effect of IFI30 on PTGS2 expression. Next, ChIP-qPCR further demonstrated that MAFF directly bound to the *PTGS2* promoter (Fig. 4H). The above findings indicate that MAFF is a transcription factor of PTGS2. Interestingly, further experiments revealed that IFI30-MAFF co-localized and interacted in GBM cells (Fig. 4I, J, Fig. S4C and S4D). Taken together, these results indicate that IFI30-induced MAFF binds to the PTGS2 promoter to regulate its expression.

3.5. IFI30-induced PGE2 shapes macrophage by binding to EP2/4 receptor

The prevailing consensus indicates that high levels of PTGS2 and its catalyzed product, PGE2, in the TME of various solid tumors have pro-tumorigenic effects, promoting the formation of immunosuppressive microenvironment by affecting diverse immune cell populations[35]. PGE2 regulates downstream pathways by binding to macrophage-surface receptors (EP1−4), encouraging macrophage migration within the TME, M2-polarization, and expression of various cytokines and chemokines[36−38]. Among the four receptors, EP1 displays the lowest affinity for PGE2[35]. We further aimed to delineate the downstream mechanism of IFI30 remodeling macrophages, several EPs and downstream pathways were tested. Tumor cell-intrinsic IFI30 was proven to drive the expression of EP2 and EP4 in macrophages (Fig. 5A and B). In addition, M-CSF is another chemoattractant for macrophages, acting on the CSF-1R to activate the downstream ERK1/2 pathway and boost the recruitment of macrophages. Previous studies have shown that PGE2-activated EPs also signal by inducing phosphorylation and activation of receptor tyrosine kinase (RTK)[39,40]. Surprisingly, in this study, overexpression of IFI30 in GBM cells was found to increase the phosphorylation levels of CSF-1R, SRC and ERK1/2 in macrophages (Fig. 5C). These data imply that IFI30 in GBM cells upregulates the EP2/EP4 on macrophages and further induces

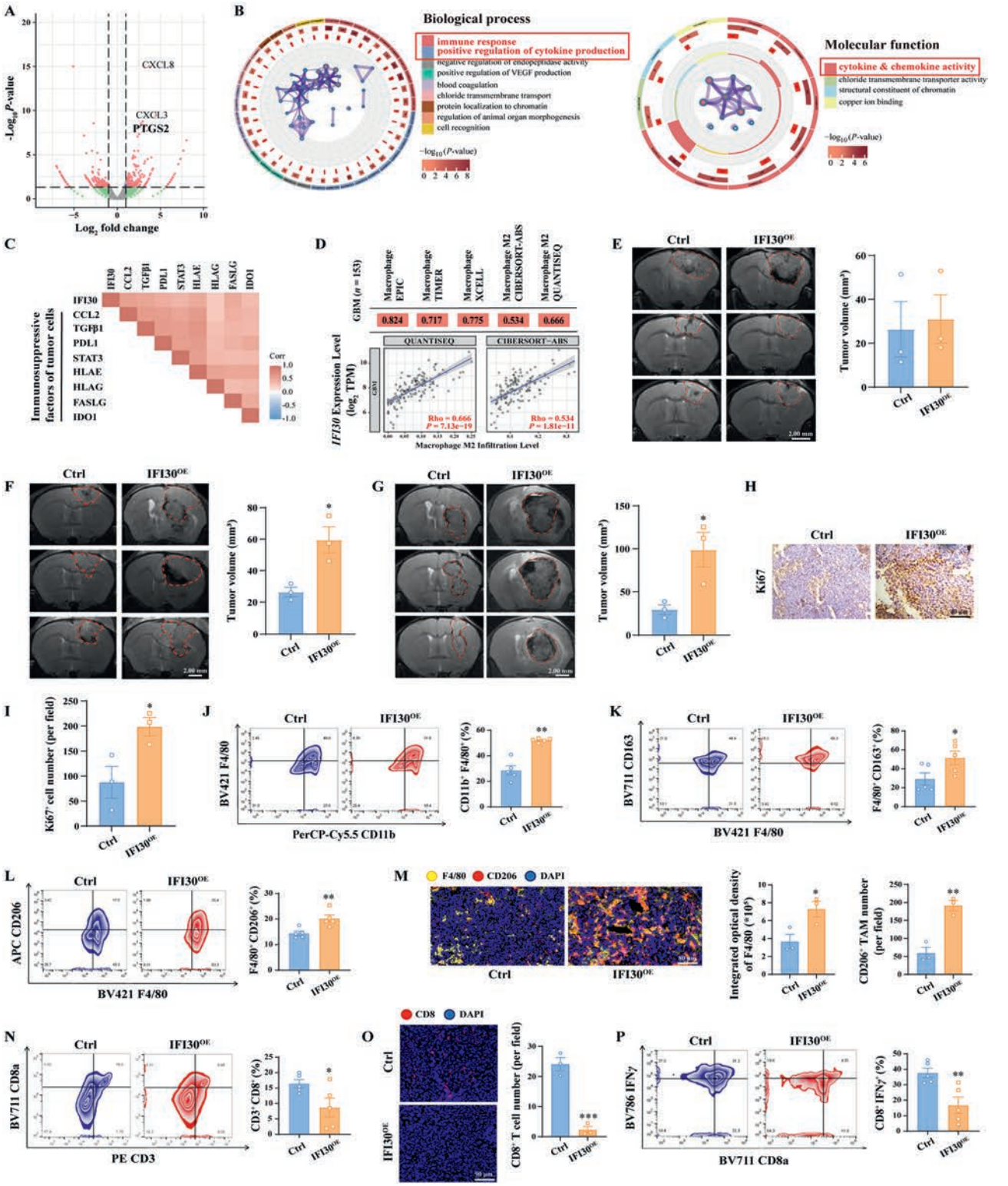

Figure 2 IFI30 is involved in immunosuppressive pathway for GBM progression. (A) Visualization of DEGs by volcano plot in U87 cells. (B) GO enrichment was performed in terms of biological process and molecular function. (C) Correlation coefficient plot showing the relationship between IFI30 and common immunosuppressive factors in the TCGA−GBM dataset. (D) IFI30 was closely related to the infiltration of M2-macrophages. (E) Representative MRI images and tumor volume of GL261 orthotopic NOD/SCID mice model. (F) Representative MRI images and tumor volume of GL261 orthotopic BALB/c-nude mice model. (G) Representative MRI images and tumor volume of GL261 orthotopic C57 mice model. (H, I) IHC analysis of Ki67 in GBM tissues of GL261 orthotopic C57 mice model (Scale bar = 40 μm). (J−M) Analyses of macrophage infiltration in IFI30 overexpression tumors. Shown are flow cytometry analyses of the $CD11b^{+}F4/80^{+}$ cells (J), $F4/80^{+}CD163^{+}$ cells (K), $F4/80^{+}CD206^{+}$ cells (L); CD206 and F4/80 staining of the tumors (M, Scale bar = 80 μm). (N−P) Analyses of T cell infiltration in IFI30 overexpression tumors. Shown are flow cytometry analysis of the $CD3^{+}CD8^{+}$ cells (N), CD8 staining of the tumors (O, Scale bar = 90 μm), flow cytometry analysis of the $CD8^{+}INF\gamma^{+}$ cells (P). Data are mean ± SEM of at least triplicate experiments. $^{***}P < 0.001$, $^{**}P < 0.01$, $^{*}P < 0.05$.

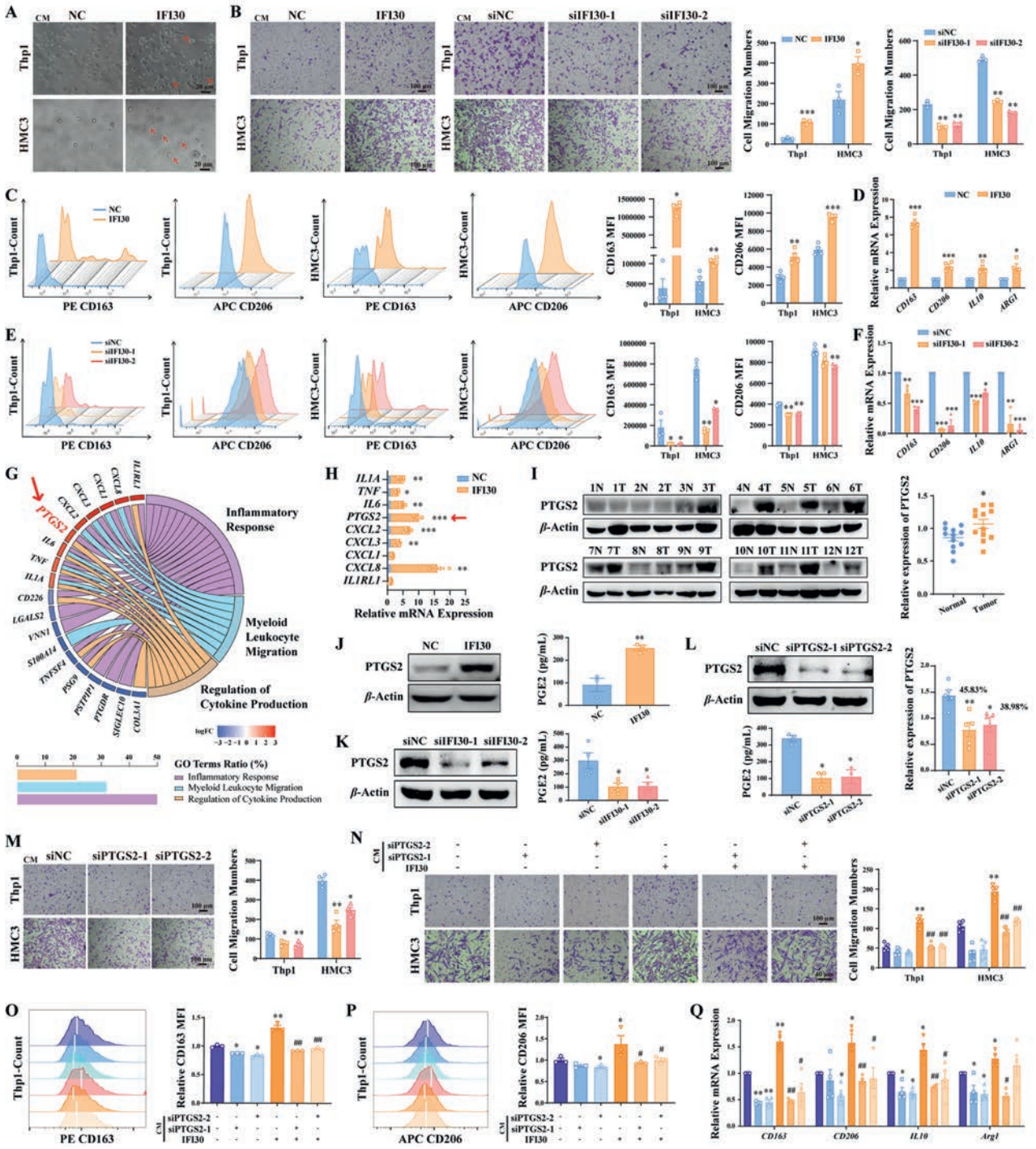

Figure 3 IFI30 induces PTGS2 expression in GBM cells to coordinate macrophages. (A) Overexpression of IFI30 in U87 cells altered macrophage morphology (Scale bar = 20 μm). (B) Transwell experiments showed that overexpression/knockdown of IFI30 in U87/U251 cells affected macrophage migration (Scale bar = 100 μm). (C, D) Overexpression of IFI30 in U87 cells increased the expression of M2 markers in macrophages. Shown are flow cytometry analyses of CD163 and CD206 (C), and RT-qPCR analyses of additional M2 markers (D). (E, F) Knockdown of IFI30 in U251 cells inhibited the expression of M2 markers in macrophages. Shown are flow cytometry analyses of CD163 and CD206 (E), and RT-qPCR analyses of additional M2 markers (F). (G) The GO terms in RNA-seq were screened to identify tumor immune-related genes regulated by IFI30. (H) Quantification of mRNA levels of *IL1A*, *TNF*, *IL6*, *PTGS2*, *CXCL2*, *CXCL3*, *CXCL1*, *CXCL8* and *IL1RL1* in U87 cells using RT-qPCR. (I) The expression of PTGS2 was higher in tumor tissues (T) than in adjacent normal brain tissues (N) of GBM patients. (J) The expression of PTGS2 and PEG2 was increased in U87-IFI30 cells. (K) The expression of PTGS2 and PEG2 was decreased in U251-siIFI30s cells. (L) The expression of PTGS2 and PEG2 was decreased in U251 cells after knockdown of PTGS2. (M) Silencing of PTGS2 in U251 cells suppressed macrophage migration measured by Transwell experiments (Scale bar = 100 μm). (N−Q) Silencing of PTGS2 in U87-IFI30 cells suppressed IFI30-induced macrophage migration and polarization. Shown are Transwell experiments (N, Scale bar = 100 and 40 μm),

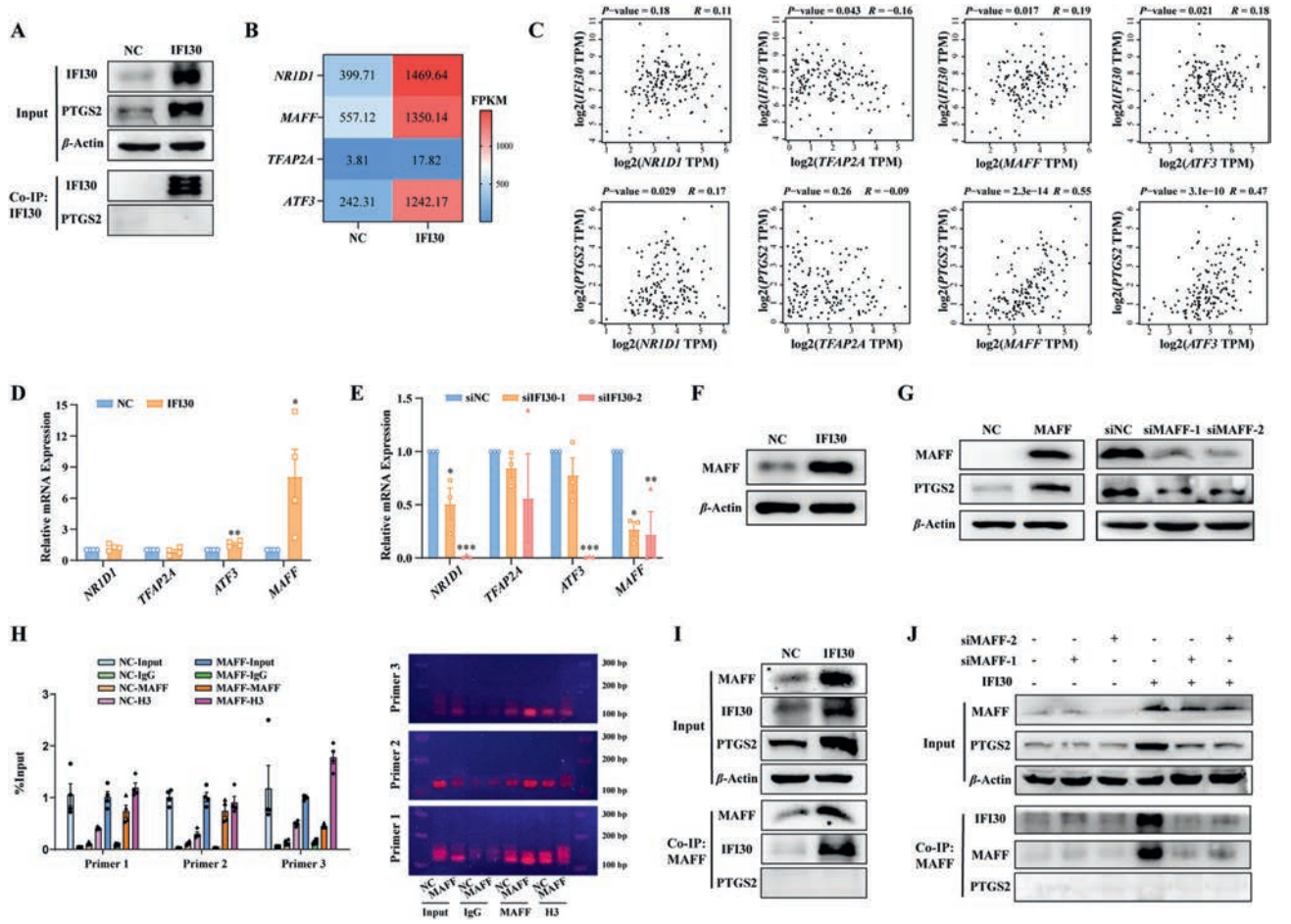

Figure 4 IFI30 enhances PTGS2 expression through the transcription factor MAFF. (A) Co-IP analysis showed that IFI30 and PTGS2 did not co-immunoprecipitate in U87 cells. (B) After overexpression of IFI30 in U87 cells, the expression of *NR1D1*, *MAFF*, *TFAP2A* and *ATF3* was analyzed using RNA-seq. (C) *In silico* analysis of TCGA data showed that *IFI30* and *PTGS2* were positively correlated with *MAFF* and *ATF3*. (D, E) Quantification of mRNA levels of *NR1D1*, *MAFF*, *TFAP2A* and *ATF3* using RT-qPCR in U87/U251 cells. (F) Protein expression of MAFF in U87-IFI30 cells. (G) Protein expression of MAFF and PTGS2 in U87-MAFF/U251-siMAFFs cells. (H) ChIP-qPCR analysis showed that MAFF was enriched in the promoter of *PTGS2* in U87 cells. (I, J) Co-IP assay showed that IFI30 and MAFF co-immunoprecipitated in U87 cells. Data are mean ± SEM of at least triplicate experiments. $^{***}P < 0.001$, $^{**}P < 0.01$, $^{*}P < 0.05$.

synergistic activation of CSF-1R through SRC-mediated crosstalk, ultimately co-promoting the migration of macrophages through the ERK1/2 pathway.

Additionally, we noticed that overexpression of IFI30 in GBM cells also raised the *p*-CREB/CREB ratio and KLF4 expression in macrophages, and facilitated the phosphorylation and nuclear translocation of STAT6 (Fig. 5D and E). Partial co-localization between p-STAT6 and KLF4 was also observed (Fig. 5F). The above findings demonstrate that IFI30 in GBM cells promotes transcriptional activation of M2 macrophage-specific genes through STAT6 and CREB-mediated KLF4 synergistically. To establish that PTGS2 and its catalytic product PGE2 are responsible for IFI30-induced signaling of macrophage recruitment and polarization, PTGS2 expression was knocked down in U87-IFI30 cells. Rescue experiments confirmed that silencing PTGS2 attenuated the effects of IFI30 in boosting EP2/EP4 expression and activating the downstream ERK1/2 and KLF4/STAT6 pathways in macrophages (Fig. 5G—I). In summary, IFI30-induced PGE2 binds to macrophage EP2/EP4 and activates the downstream ERK1/2 and KLF4/STAT6 pathways, leading to macrophage recruitment and polarization.

3.6. IFI30-overexpression-induced pro-tumorigenic properties are abolished after TAMs depletion and PTGS2 inhibition

Given the substantial rise in the infiltration of TAMs after overexpression of IFI30 *in vivo* and *in vitro*, an *in situ* TAMs depletion test was carried out to provide additional confirmation of the role of TAMs in IFI30-induced GBM progression. Briefly, GL261-IFI30^{OE} and GL261-Ctrl cells were injected into the striatum of C57 mice, and then clodronate liposome was used to deplete macrophages and microglia from the GBM microenvironment (Fig. 6A, Supporting Information Fig. S5A). Whereas, *in situ* depletion of macrophages by encapsulated clodronate eliminated the differences in tumor

flow cytometry analyses of CD163 (O) and CD206 (P), and RT-qPCR analyses of additional M2 markers (Q). Data are mean ± SEM of at least triplicate experiments. $^{***}P < 0.001$, $^{**}P < 0.01$, $^{*}P < 0.05$ *vs* NC group; $^{\#\#}P < 0.01$, $^{\#}P < 0.05$ *vs* IFI30^{OE} group.

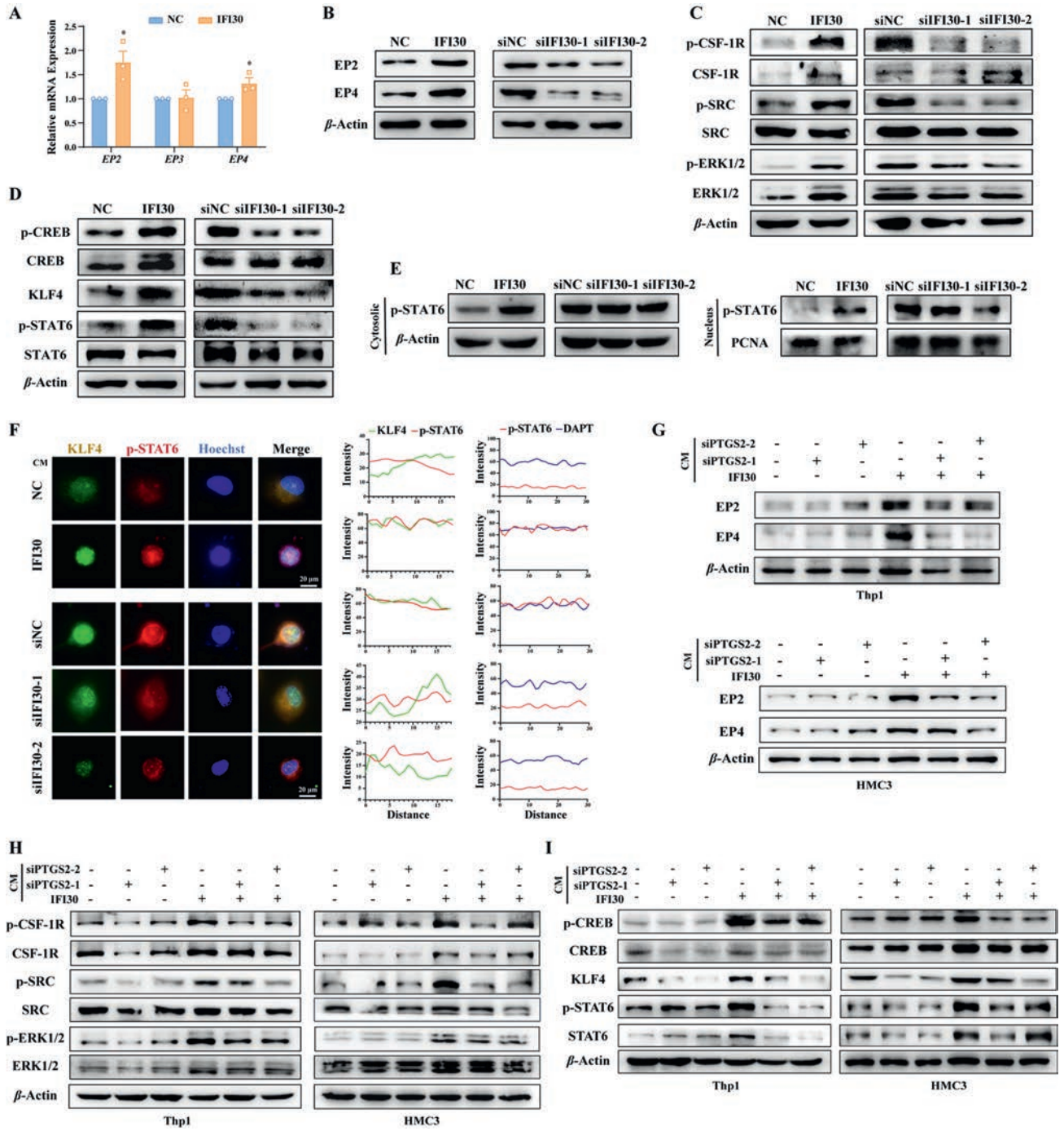

Figure 5 IFI30-induced PGE2 shapes macrophage by binding to EP2/4 receptor. (A) Overexpression of IFI30 in U87 cells encouraged the mRNA expression of *EP2* and *EP4* in macrophages. (B−D) The effects of overexpression/knockdown of IFI30 in U87/U251 cells on the expression of corresponding proteins in macrophages. (E) The effect of overexpression/knockdown of IFI30 in U87/U251 cells on cytosolic and nuclear expression of p-STAT6 in macrophages. (F) Immunofluorescence images of KLF4 and p-STAT6 in macrophages (Scale bar = 20 μm). (G−I) Western blot results showed that silencing PTGS2 impaired the effects of IFI30 on the expression of EP2/EP4, and the activation of downstream ERK1/2 and KLF4/STAT6 pathways in macrophages. Data are mean ± SEM of at least triplicate experiments. $*P < 0.05$.

progression induced by IFI30 overexpression, the tumors initiated and grew at similar rates in the $IFI30^{OE}$/Ctrl groups (Fig. 6B and C). Altogether, these data indicate that the effect of IFI30 on the progression of GBM depends largely on the modulation of TAMs.

Finally, we sought to determine whether pharmacological inhibition of PTGS2 *in vivo* would affect the IFI30-induced growth and immunosuppression of the tumor (Fig. 6A). Here, we found that celecoxib treatment inhibited IFI30-induced tumor growth (Fig. 6B and C). Celecoxib suppressed the infiltration of M2-TAMs in IFI30-

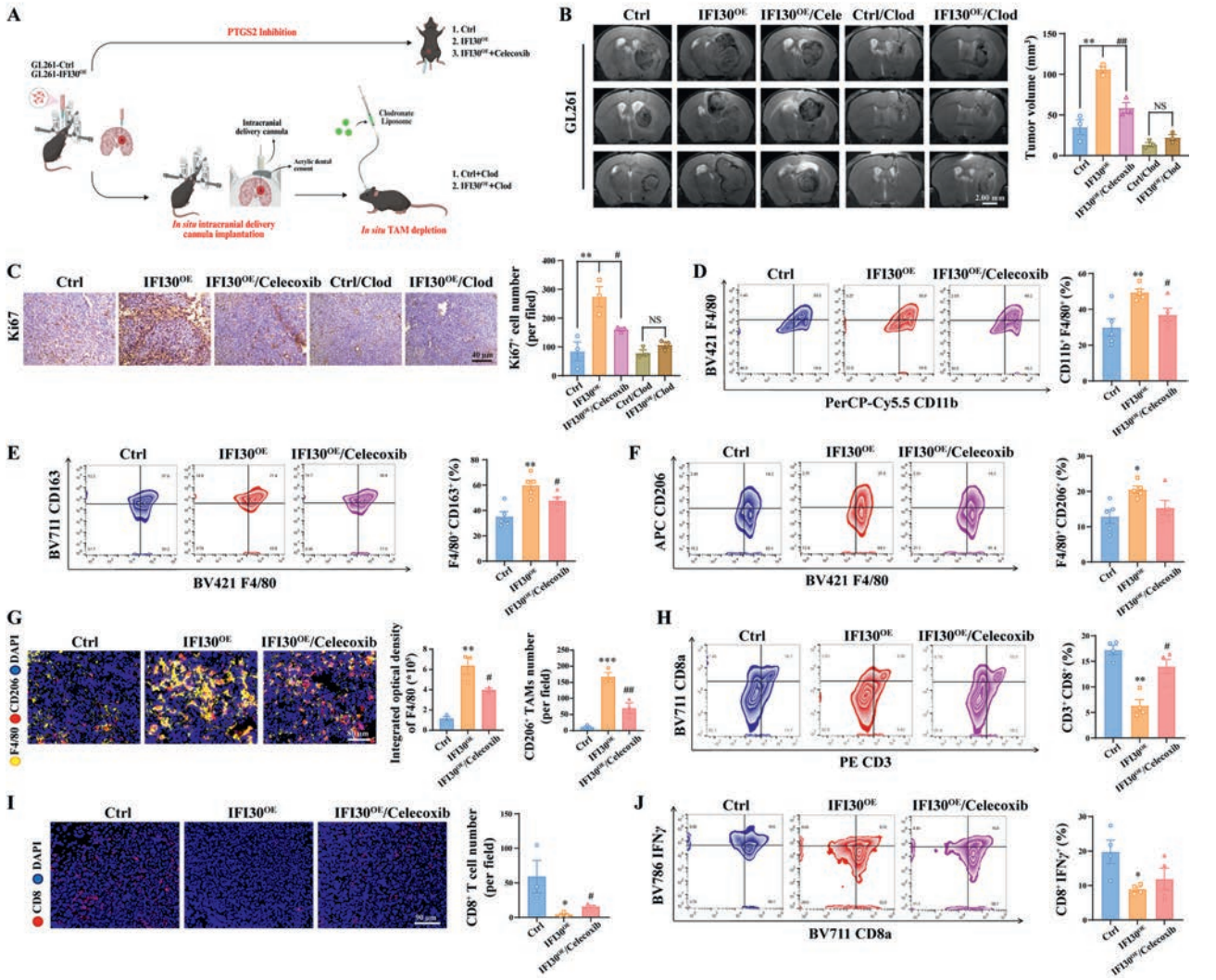

Figure 6 IFI30-overexpression-induced pro-tumorigenic properties are abolished after TAMs depletion and PTGS2 inhibition. (A) Schematic diagram of constructing the GBM orthotopic model and the *in situ* TAM depletion model in C57 mice. (B) After TAMs depletion and PTGS2 inhibition, IFI30-induced tumor growth in mice was abolished. (C) IHC results of Ki67 in GBM tissues of GL261 orthotopic C57 mice model (Scale bar = 40 μm). (D−G) Analyses of macrophage infiltration in IFI30-overexpressing tumors treated with celecoxib. Shown are flow cytometry analysis of the $CD11b^{+}F4/80^{+}$ cells (D), $F4/80^{+}CD163^{+}$ cells (E), $F4/80^{+}CD206^{+}$ cells (F); CD206 and F4/80 staining of the tumors (G, Scale bar = 80 μm). (H−J) Analyses of T cell infiltration in IFI30-overexpressing tumors treated with celecoxib. Shown are flow cytometry analyses of the $CD3^{+}CD8^{+}$ cells (H), $CD8^{+}INF\gamma^{+}$ cells (J), and CD8 staining of the tumors (I, Scale bar = 90 μm). Data are mean ± SEM of at least triplicate experiments. $^{***}P < 0.001$, $^{**}P < 0.01$, $^{*}P < 0.05$ *vs* Ctrl group; $^{\#\#}P < 0.01$, $^{\#}P < 0.05$ *vs* $IFI30^{OE}$ group; NS, not significant.

overexpressing tumors, but did not alter the infiltration and function of $CD4^{+}/CD8^{+}$ T cells (Fig. 6D−J and Fig. S5B−S5D).

All in all, our results suggest that IFI30 promotes the progression of GBM mainly by coordinating TAMs to participate in the immunosuppressive microenvironment through the PTGS2/PGE2 pathway.

4. Discussion

GBM is one of the most malignant brain tumors. Despite the application of standard multimodality therapies including surgery, radiotherapy and chemotherapy (Temozolomide), the median survival is still only 8 months[41], and the recurrence rate is close to 100%. Exploring new therapeutic strategies for GBM is the utmost urgent need. The current discovery of the intracranial lymphatic system has overturned the perception of the brain as "immunologically privileged" and established a new awareness of the intracranial infiltration and function of TME[42,43]. The unique immune microenvironment infiltrated by high M2-TAMs in GBM interferes with the cytotoxic function of T cells[44]. Therefore, targeting TAMs[45] is expected to improve the prognosis of patients with GBM by reversing "immune cold" TME to "immune normalized" TME. Indeed, the intrinsic properties of heterogeneous cancer cells fundamentally regulate the host immune response and the infiltration of TAMs. In the study, our data propose a mechanism of IFI30 that may underlie the crosstalk between GBM cells and TAMs. In GBM, enhanced histone modifications H3K4me3 and H3K27ac were involved in the

overexpression of IFI30, which was correlated with immunosuppression and tumor progression. We uncovered that the beneficial effects of IFI30 on GBM may be mediated by modulating the antitumor immune responses. IFI30 induced PGE2 expression in GBM cells *via* the MAFF/PTGS2 axis. PGE2 binds to macrophage EP2/EP4, regulating macrophage phenotype and infiltration. Our results indicated that IFI30 is a novel, potential tumor therapeutic target that urgently needs to be explored.

The internal regulatory mechanisms of IFI30 abnormal expression in GBM, especially epigenetic regulation, are not yet known. In this study, we confirmed through ChIP-qPCR combined with multiple inhibitors that the epigenetic gains of H3K4me3 and H3K27Ac at the promoter were required for activation of IFI30. Two prominent histone lysine modifications (H3K27ac and H3K4me3) are predominantly enriched and overlap in the promoter and enhancer regions of actively transcribed genes[46,47], collectively promoting gene activation for expression, which can be crucial in tumor progression, immune escape and drug resistance[48–52]. H3K4me3-gain and H3K27ac-gain were also found in IFI30-upregulated GBM tissues. However, the specific regulatory enzymes involved in IFI30 histone modification were not delved into in this study, which still needs to be supplemented and improved in future studies.

Previous *in silico* studies preliminarily revealed that IFI30 reflected the progression of GBM by inducing the infiltration of immune cells and modulating the immunosuppressive TME[30,31], but experimental support for this hypothesis is currently lacking. In this study, we demonstrated through immunocompetent and immunodeficient mice models with orthotopic tumors, that the GBM-promoting effects of IFI30 were probably associated with immune-related variables in the TME. Notably, through *in vivo*/*in vitro* experiments, we found that IFI30 enhanced the infiltration of TAMs, and depressed the proportion of $CD8^+$ T cells. Compared with $CD8^+$ T cells, TAMs exhibit more abundant infiltration in GBM patients[53,54], reflecting the game between antitumor immunity and immunosuppression. TAMs are also regarded as a poor prognostic marker of GBM[55,56], promoting diffuse growth and recurrence of tumor[57,58]. In addition, TAMs can directly or indirectly inhibit the proliferation and killing functions of $CD8^+$ T cells and promote their depletion through various mechanisms. Targeted depletion of TAMs from the GBM immune microenvironment eliminated the contribution of IFI30 to tumor progression in C57 mice, suggesting that the pro-tumor effects of IFI30 largely depend on TAMs.

PTGS2 mediates the initial committed step in prostanoid synthesis by converting arachidonic acid to PGE2[59]. Normally, basal expression levels of PTGS2 are low or absent, but it is induced in cancerous tissues, including GBM[60]. PTGS2 and its product, PGE2, actively contribute to tumor immune escape by stimulating pro-tumoral phenotype differentiation and infiltration into the TME of multiple immune cells, such as TAMs, dendritic cells, and T cells. Previous studies have shown that targeting

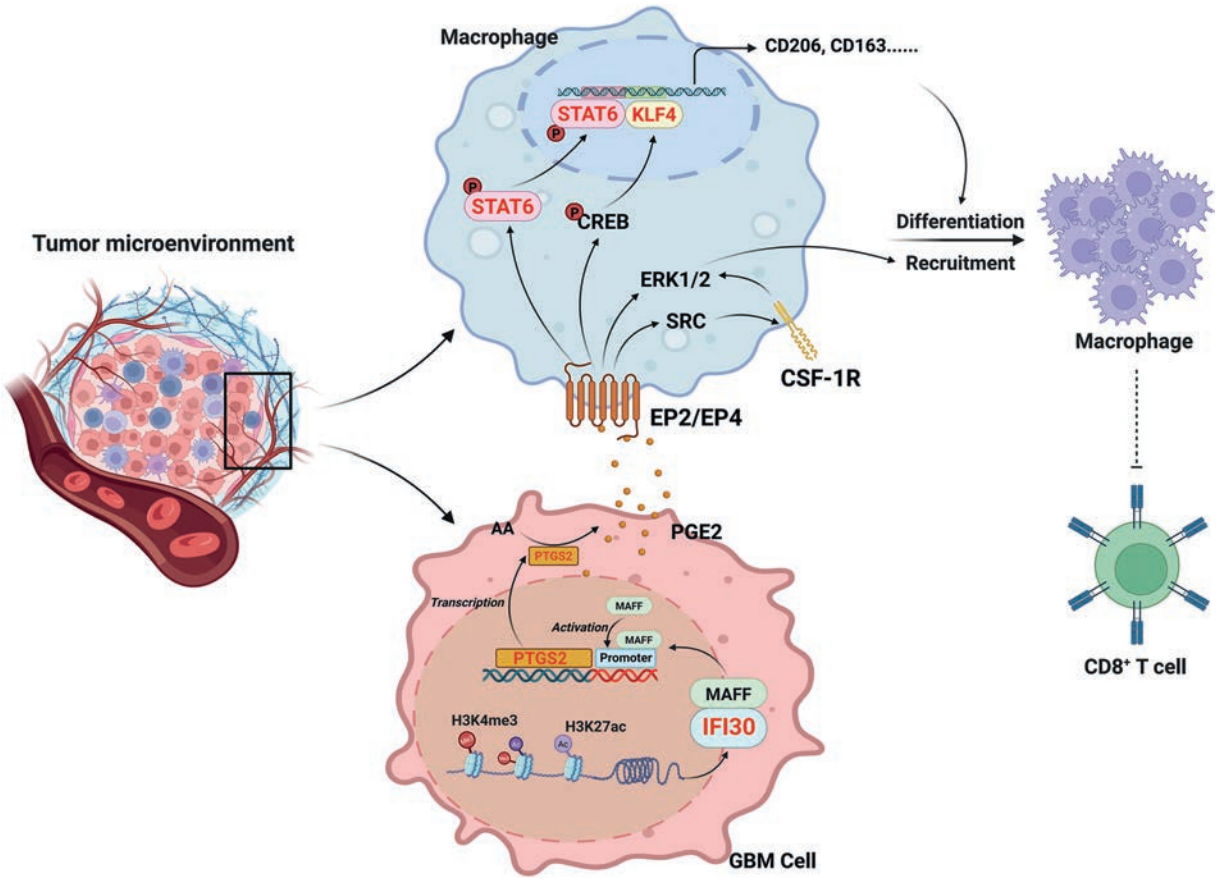

Figure 7 Diagram showing the proposed mechanism of IFI30 in the GBM immune microenvironment. IFI30 is highly expressed in GBM and regulated by histone modifications H3K4me3 and H3K27ac. IFI30 induces the expression of PGE2 through the MAFF/PTGS2 pathway in GBM cells. PGE2 binds to macrophage EP2/EP4 and activates the downstream ERK1/2 and KLF4/STAT6 pathways, stimulating the TAMs infiltration and GBM progression.

PTGS2 in pancreatic cancer[61], breast cancer[62], and melanoma[63] could alleviate immunosuppression and inhibit tumor growth. We further investigated the mechanism and found that IFI30 drove the expression of PTGS2 and PGE2 in GBM cells. Treatment with celecoxib, an inhibitor of PTGS2, reduced M2-TAMs infiltration in the $IFI30^{OE}$ group of mice, suppressing tumor growth. In addition, we first discovered and characterized MAFF as the PTGS2 transcription factor. MAFF is a member of the MAF family of basic region leucine zipper (bZIP)-type transcription factors and can be involved in the tumor immunosuppressive microenvironment by controlling inflammation-related gene expression. A recent study reports that MAFF intervenes in the recruitment and maturation of macrophage and granulocyte by stimulating the expression of CXCL1 and CSF3[64]. Also, our *in silico* analysis and ChIP-qPCR data proved that IFI30-induced transcription factor MAFF bound to the PTGS2 promoter to regulate its expression.

The primary biological function of PGE2 in inflammation-associated cancer was mediated by four G-protein-coupled PGE2 receptors (GPCR, EP) (EP1−4). EP2 and EP4 are the EPs predominantly expressed by human macrophages[65], mediating the function of PGE2 signaling[36,66]. A previous study showed that activated EP2/EP4 promotes macrophage migration through the downstream ERK1/2 signaling[38]. In the present study, we found that IFI30 activated the EP2/EP4 and downstream ERK1/2 pathways of macrophages by inducing PTGS2 and PGE2 expression, facilitating the migration of macrophages. PGE2-activated EPs are also known to signal by evoking the phosphorylation of RTK. In human oral squamous cell carcinoma cell line SCC-9, PGE2/EP2 signaling enhances iNOS expression by transactivating the EGF receptor *via* the SRC pathway[39]. Surprisingly, we detected that overexpression of IFI30 in GBM cells triggered the phosphorylated activation of CSF-1R in macrophages, which may be attributed to the crosstalk between EP2/EP4 and CSF-1R through the SRC pathway. CSF-1R, as an RTK, maintains the survival, proliferation, and motility of monocyte/macrophage through several downstream signaling pathways including ERK1/2[67]. Our results revealed that IFI30-induced PGE2 activated macrophage EP2/EP4, which caused transactivation of CSF-1R *via* the SRC pathway, synergistically attracting the recruitment of macrophage within the TME through the ERK1/2 pathway.

As GPCRs, EP2/EP4 mediates the anti-inflammatory activity of PGE2 through the cAMP/CREB pathway[65]. Although CREB is necessary for the expression of PGE2-induced M2-marker genes, the absence of conserved CREB binding sites on the promoter of these genes points to the involvement of additional transcriptional activators in mediating these effects. Our previous investigation revealed that KLF4 is an evolutionarily conserved zinc-finger-containing transcription factor, whose promoter contains CREB binding sites[68,69] at −269 and −232 relative to the transcription start site, suggesting that PGE2 may induce KLF4 expression through the CREB pathway. KLF4 has been shown to cooperate with STAT6 in promoting M2-polarization of macrophages. KLF4 deficiency disrupts the function of M2-macrophages and increases the expression of proinflammatory genes[70]. The STAT6 pathway is very critical to M2-polarization of macrophages[71] and mediates the transcriptional activation of M2 macrophage-specific genes[72]. Jinglin Wang et al.[73] found that mesenchymal stem cell-derived PGE2 induced M2-polarization of macrophages by activating the EP4/STAT6 pathway. Liao et al.[70] demonstrated that KLF4 is both induced by and cooperates with STAT6, and that the intact KLF4 site is required for maximal transcriptional activity of STAT6 (and *vice versa*). Furthermore, in this study, IFI30-induced PGE2 acted on EP2/EP4 to stimulate M2-polarization of macrophages *via* STAT6 and CREB/KLF4 pathway. A representative mechanism diagram is shown in Fig. 7.

5. Conclusions

The expression of IFI30 varies in different cancers, which indicates that the expression pattern and function of IFI30 are heterogeneous in different cancers and may be highly dependent on the immunogenicity and immunosuppressive microenvironment of the tumor. The unified characteristics and mechanism of IFI30 under pan-cancer still need to be further explored. This study focuses on the non-immunogenic tumor-GBM, revealing the critical role of IFI30 in regulating GBM progression. IFI30 was highly expressed in GBM, regulated by H3K4me3 and H3K27ac. In the GBM immune microenvironment, IFI30 induced the expression of PGE2 in GBM cells through the MAFF/PTGS2 pathway, and PGE2 bound to macrophage EP2/EP4, activating the downstream ERK1/2 and KLF4/STAT6 pathways, which stimulated the TAMs infiltration and GBM progression. In summary, IFI30 may become an important R&D target for GBM therapy.

Acknowledgments

This work was supported Beijing Natural Science Foundation (Nos. 7252202 and 25JL008, China), National Natural Science Foundation of China (82304523), CAMS Innovation Fund for Medical Sciences (2021-I2M-1-029 and 2023-I2M-2-006, China).

Author contributions

Jinhua Wang: conceptualization, supervision, funding acquisition, writing - review & Editing; Yu Wang: conceptualization, supervision, resources. Jie Yi: resources; Sen Zhang, Wenlin Chen: investigation, writing-original draft; Wan Li, Yihui Yang: validation, formal analysis; Liwen Ren, Xiangjin Zheng, Hong Yang: validation, methodology; Guanhua Du: supervision, funding acquisition.

Conflicts of interest

The authors declare no conflicts of interest.

Appendix A. Supporting information

Supporting information to this article can be found online at https://doi.org/10.1016/j.apsb.2026.06.002.

References

1. Chen R, Smith Cohn M, Cohen AL, Colman H. Glioma subclassifications and their clinical significance. *Neurotherapeutics* 2017; **14**:284−97.
2. Hodi FS, O'Day SJ, McDermott DF, Weber RW, Sosman JA, Haanen JB, et al. Improved survival with ipilimumab in patients with metastatic melanoma. *N Engl J Med* 2010;**363**:711−23.
3. Motzer R, Alekseev B, Rha SY, Porta C, Eto M, Powles T, et al. Lenvatinib plus pembrolizumab or everolimus for advanced renal cell carcinoma. *N Engl J Med* 2021;**384**:1289−300.
4. Nayak L, Molinaro AM, Peters K, Clarke JL, Jordan JT, de Groot J, et al. Randomized phase II and biomarker study of pembrolizumab

plus bevacizumab *versus* pembrolizumab alone for patients with recurrent glioblastoma. *Clin Cancer Res* 2021;**27**:1048−57.
5. Yang T, Kong Z, Ma W. PD-1/PD-L1 immune checkpoint inhibitors in glioblastoma: clinical studies, challenges and potential. *Hum Vaccines Immunother* 2021;**17**:546−53.
6. Lim M, Xia Y, Bettegowda C, Weller M. Current state of immunotherapy for glioblastoma. *Nat Rev Clin Oncol* 2018;**15**:422−42.
7. Qiu Q, Chen S, He H, Chen J, Ding X, Wang D, et al. An injectable signal-amplifying device elicits a specific immune response against malignant glioblastoma. *Acta Pharm Sin B* 2023;**13**:5091−106.
8. Jang Y, Choi J, Park B, Park JY, Lee JH, Goo J, et al. Activatable PROTAC nanoassembly for photodynamic PTP1B proteolysis enhances glioblastoma immunotherapy. *Acta Pharm Sin B* 2025;**15**:4886−99.
9. Mohme M, Neidert MC, Regli L, Weller M, Martin R. Immunological challenges for peptide-based immunotherapy in glioblastoma. *Cancer Treat Rev* 2014;**40**:248−58.
10. Wen PY, Weller M, Lee EQ, Alexander BM, Barnholtz Sloan JS, Barthel FP, et al. Glioblastoma in adults: a Society for Neuro-Oncology (SNO) and European Society of Neuro-Oncology (EANO) consensus review on current management and future directions. *Neuro Oncol* 2020;**22**:1073−113.
11. Gutmann DH, Kettenmann H. Microglia/brain macrophages as central drivers of brain tumor pathobiology. *Neuron* 2019;**104**:442−9.
12. Stein M, Keshav S, Harris N, Gordon S. Interleukin 4 potently enhances murine macrophage mannose receptor activity: a marker of alternative immunologic macrophage activation. *J Exp Med* 1992;**176**: 287−92.
13. Goerdt S, Orfanos CE. Other functions, other genes: alternative activation of antigen-presenting cells. *Immunity* 1999;**10**:137−42.
14. Mills CD, Kincaid K, Alt JM, Heilman MJ, Hill AM. M-1/M-2 macrophages and the Th1/Th2 paradigm. *J Immunol* 2000;**164**: 6166−73.
15. Biswas SK, Mantovani A. Macrophage plasticity and interaction with lymphocyte subsets: cancer as a paradigm. *Nat Immunol* 2010;**11**: 889−96.
16. Qian BZ, Pollard JW. Macrophage diversity enhances tumor progression and metastasis. *Cell* 2010;**141**:39−51.
17. Jackson CM, Choi J, Lim M. Mechanisms of immunotherapy resistance: lessons from glioblastoma. *Nat Immunol* 2019;**20**:1100−9.
18. Liu YY, Yao RQ, Long LY, Liu YX, Tao BY, Liu HY, et al. Worldwide productivity and research trend of publications concerning glioma-associated macrophage/microglia: a bibliometric study. *Front Neurol* 2022;**13**:1047162.
19. O'Donnell PW, Haque A, Klemsz MJ, Kaplan MH, Blum JS. Cutting edge: induction of the antigen-processing enzyme IFN-γ-inducible lysosomal thiol reductase in melanoma cells is STAT1-dependent but CIITA-independent. *J Immunol* 2004;**173**:731−5.
20. Hastings KT. GILT: shaping the MHC class II-restricted peptidome and $CD4^+$ T cell-mediated immunity. *Front Immunol* 2013;**4**:429.
21. Hastings KT, Lackman RL, Cresswell P. Functional requirements for the lysosomal thiol reductase GILT in MHC class II-restricted antigen processing. *J Immunol* 2006;**177**:8569−77.
22. Chen S, Wang Q, Shao X, Di G, Dai Y, Jiang X, et al. Lentivirus mediated γ-interferon-inducible lysosomal thiol reductase (GILT) knockdown suppresses human glioma U373MG cell proliferation. *Biochem Biophys Res Commun* 2019;**509**:182−7.
23. Phipps Yonas H, Cui H, Sebastiao N, Brunhoeber PS, Haddock E, Deymier MJ, et al. Low GILT expression is associated with poor patient survival in diffuse large B-cell lymphoma. *Front Immunol* 2013; **4**:425.
24. Hathaway Schrader JD, Norton D, Hastings K, Doonan BP, Fritz ST, Bethard JR, et al. GILT expression in human melanoma cells enhances generation of antigenic peptides for HLA class II-mediated immune recognition. *Int J Mol Sci* 2022;**23**:1066.
25. Adams AC, Borden ES, Macy AM, Thomson N, Cui H, Gimbel MI, et al. High GILT expression is associated with improved survival in metastatic melanoma patients treated with immune checkpoint inhibition. *Cancers* 2022;**14**:2200.
26. Nguyen J, Bernert R, In K, Kang P, Sebastiao N, Hu C, et al. Gamma-interferon-inducible lysosomal thiol reductase is upregulated in human melanoma. *Melanoma Res* 2016;**26**:125−37.
27. Ye C, Zhou W, Wang F, Yin G, Zhang X, Kong L, et al. Prognostic value of gamma-interferon-inducible lysosomal thiol reductase expression in female patients diagnosed with breast cancer. *Int J Cancer* 2022;**150**:705−17.
28. Xiang YJ, Guo MM, Zhou CJ, Liu L, Han B, Kong LY, et al. Absence of gamma-interferon-inducible lysosomal thiol reductase (GILT) is associated with poor disease-free survival in breast cancer patients. *PLoS One* 2014;**9**:e109449.
29. Buetow KH, Meador LR, Menon H, Lu YK, Brill J, Cui H, et al. High GILT expression and an active and intact MHC class II antigen presentation pathway are associated with improved survival in melanoma. *J Immunol* 2019;**203**:2577−87.
30. Zhu C, Chen X, Guan G, Zou C, Guo Q, Cheng P, et al. IFI30 is a novel immune-related target with predicting value of prognosis and treatment response in glioblastoma. *OncoTargets Ther* 2020;**13**: 1129−43.
31. Liu X, Song C, Yang S, Ji Q, Chen F, Li W. IFI30 expression is an independent unfavourable prognostic factor in glioma. *J Cell Mol Med* 2020;**24**:12433−43.
32. Ye J, Xu W, Chen T. Knockdown of interferon-γ inducible protein 30 (IFI30) inhibits the proliferation, invasion and migration of human glioma U251 cells by activating STAT1 and promotes their apoptosis. *Cell Mol Immunol* 2024;**40**:33−42.
33. Yin X, Wu Q, Hao Z, Chen L. Identification of novel prognostic targets in glioblastoma using bioinformatics analysis. *Biomed Eng Online* 2022;**21**:26.
34. Holliday R. The inheritance of epigenetic defects. *Science* 1987;**238**: 163−70.
35. Santiso A, Heinemann A, Kargl J. Prostaglandin E2 in the tumor microenvironment, a convoluted affair mediated by EP receptors 2 and 4. *Pharmacol Rev* 2024;**76**:388−413.
36. Chen Z, Yang Y, Neo SY, Shi H, Chen Y, Wagner AK, et al. Phosphodiesterase 4A confers resistance to PGE2-mediated suppression in $CD25^+$/$CD54^+$ NK cells. *EMBO Rep* 2021;**22**:e51329.
37. Tang EHC, Libby P, Vanhoutte PM, Xu A. Anti-inflammation therapy by activation of prostaglandin EP4 receptor in cardiovascular and other inflammatory diseases. *J Cardiovasc Pharmacol* 2012;**59**:116−23.
38. Digiacomo G, Ziche M, Dello Sbarba P, Donnini S, Rovida E. Prostaglandin E2 transactivates the colony-stimulating factor-1 receptor and synergizes with colony-stimulating factor-1 in the induction of macrophage migration *via* the mitogen-activated protein kinase ERK1/2. *FASEB J* 2015;**29**:2545−54.
39. Donnini S, Finetti F, Solito R, Terzuoli E, Sacchetti A, Morbidelli L, et al. EP2 prostanoid receptor promotes squamous cell carcinoma growth through epidermal growth factor receptor transactivation and iNOS and ERK1/2 pathways. *FASEB J* 2007;**21**:2418−30.
40. Battersby S, Sales KJ, Williams AR, Anderson RA, Gardner S, Jabbour HN. Seminal plasma and prostaglandin E2 up-regulate fibroblast growth factor 2 expression in endometrial adenocarcinoma cells *via* E-series prostanoid-2 receptor-mediated transactivation of the epidermal growth factor receptor and extracellular signal-regulated kinase pathway. *Hum Reprod* 2007;**22**:36−44.
41. Ostrom QT, Cioffi G, Waite K, Kruchko C, Barnholtz Sloan JS. CBTRUS statistical report: primary brain and other central nervous system tumors diagnosed in the United States in 2014−2018. *Neuro Oncol* 2021;**23**:1−105.
42. Louveau A, Smirnov I, Keyes TJ, Eccles JD, Rouhani SJ, Peske JD, et al. Structural and functional features of central nervous system lymphatic vessels. *Nature* 2015;**523**:337−41.
43. Aspelund A, Antila S, Proulx ST, Karlsen TV, Karaman S, Detmar M, et al. A dural lymphatic vascular system that drains brain interstitial fluid and macromolecules. *J Exp Med* 2015;**212**:991−9.
44. Chongsathidkiet P, Jackson C, Koyama S, Loebel F, Cui X, Farber SH, et al. Sequestration of T cells in bone marrow in the setting of glioblastoma and other intracranial tumors. *Nat Med* 2018;**24**:1459−68.

45. Li AQ, Huang F, Talaiti S, Yang X, Bi H, Fang JH. Understanding the complexity of tumor-associated macrophages: druggable and therapeutic insights. *Acta Pharm Sin B* 2025;**15**:4456−75.
46. Beacon TH, Delcuve GP, López C, Nardocci G, Kovalchuk I, van Wijnen AJ, et al. The dynamic broad epigenetic (H3K4me3, H3K27ac) domain as a mark of essential genes. *Clin Epigenet* 2021;**13**:138.
47. Zhao W, Xu Y, Wang Y, Gao D, King J, Xu Y, et al. Investigating crosstalk between H3K27 acetylation and H3K4 trimethylation in CRISPR/dCas-based epigenome editing and gene activation. *Sci Rep* 2021;**11**:15912.
48. Pai CP, Wang H, Seachrist DD, Agarwal N, Adams JA, Liu Z, et al. The PML1−WDR5 axis regulates H3K4me3 marks and promotes stemness of estrogen receptor-positive breast cancer. *Cell Death Differ* 2024;**31**:768−78.
49. Ravindran Menon D, Hammerlindl H, Gimenez G, Hammerlindl S, Zuegner E, Torrano J, et al. H3K4me3 remodeling induced acquired resistance through *O*-GlcNAc transferase. *Drug Resist Updates* 2023; **71**:100993.
50. Liu J, Zhou WY, Luo XJ, Chen YX, Wong CW, Liu ZX, et al. Long noncoding RNA regulating immune escape regulates mixed lineage leukaemia protein-1-H3K4me3-mediated immune escape in oesophageal squamous cell carcinoma. *Clin Transl Med* 2023;**13**: e1410.
51. Zhang Y, Liu Z, Yang X, Lu W, Chen Y, Lin Y, et al. H3K27 acetylation activated-COL6A1 promotes osteosarcoma lung metastasis by repressing STAT1 and activating pulmonary cancer-associated fibroblasts. *Theranostics* 2021;**11**:1473−92.
52. Wang J, Sun Y, Zhang X, Cai H, Zhang C, Qu H, et al. Oxidative stress activates NORAD expression by H3K27ac and promotes oxaliplatin resistance in gastric cancer by enhancing autophagy flux *via* targeting the miR-433-3p. *Cell Death Dis* 2021;**12**:90.
53. González Tablas Pimenta M, Otero Á, Arandia Guzman DA, Pascual Argente D, Ruíz Martín L, Sousa Casasnovas P, et al. Tumor cell and immune cell profiles in primary human glioblastoma: impact on patient outcome. *Brain Pathol* 2021;**31**:365−80.
54. Karimi E, Yu MW, Maritan SM, Perus LJM, Rezanejad M, Sorin M, et al. Single-cell spatial immune landscapes of primary and metastatic brain tumours. *Nature* 2023;**614**:555−63.
55. Szulzewsky F, Pelz A, Feng X, Synowitz M, Markovic D, Langmann T, et al. Glioma-associated microglia/macrophages display an expression profile different from M1 and M2 polarization and highly express Gpnmb and Spp1. *PLoS One* 2015;**10**:e0116644.
56. Roesch S, Rapp C, Dettling S, Herold Mende C. When immune cells turn bad-tumor-associated microglia/macrophages in glioma. *Int J Mol Sci* 2018;**19**:436.
57. Vinnakota K, Hu F, Ku MC, Georgieva PB, Szulzewsky F, Pohlmann A, et al. Toll-like receptor 2 mediates microglia/brain macrophage MT1−MMP expression and glioma expansion. *Neuro Oncol* 2013;**15**:1457−68.
58. Pyonteck SM, Akkari L, Schuhmacher AJ, Bowman RL, Sevenich L, Quail DF, et al. CSF-1R inhibition alters macrophage polarization and blocks glioma progression. *Nat Med* 2013;**19**:1264−72.
59. Dean PT, Hooks SB. Pleiotropic effects of the COX-2/PGE2 axis in the glioblastoma tumor microenvironment. *Front Oncol* 2022;**12**:1116014.
60. Qiu J, Shi Z, Jiang J. Cyclooxygenase-2 in glioblastoma multiforme. *Drug Discov Today* 2017;**22**:148−56.
61. Markosyan N, Li J, Sun YH, Richman LP, Lin JH, Yan F, et al. Tumor cell-intrinsic EPHA2 suppresses anti-tumor immunity by regulating PTGS2 (COX-2). *J Clin Investig* 2019;**129**:3594−609.
62. Coutinho LL, Femino EL, Gonzalez AL, Moffat RL, Heinz WF, Cheng RYS, et al. NOS2 and COX-2 co-expression promotes cancer progression: a potential target for developing agents to prevent or treat highly aggressive breast cancer. *Int J Mol Sci* 2024;**25**:6103.
63. Liu Y, He J, Li M, Ren K, Zhao Z. Inflammation-driven nanohitchhiker enhances postoperative immunotherapy by alleviating prostaglandin E2-mediated immunosuppression. *ACS Appl Mater Interfaces* 2024;**16**:6879−93.
64. Saliba J, Coutaud B, Solovieva V, Lu F, Blank V. Regulation of CXCL1 chemokine and CSF3 cytokine levels in myometrial cells by the MAFF transcription factor. *J Cell Mol Med* 2019;**23**:2517−25.
65. Ratcliffe MJ, Walding A, Shelton PA, Flaherty A, Dougall IG. Activation of E-prostanoid4 and E-prostanoid2 receptors inhibits TNF-alpha release from human alveolar macrophages. *Eur Respir J* 2007;**29**:986−94.
66. Wu JMF, Cheng YY, Tang TWH, Shih C, Chen JH, Hsieh PCH. Prostaglandin E2 receptor 2 modulates macrophage activity for cardiac repair. *J Am Heart Assoc* 2018;**7**:e009216.
67. Hamilton JA. CSF-1 signal transduction. *J Leukoc Biol* 1997;**62**: 145−55.
68. Stavri S, Simionescu M, Kardassis D, Gafencu AV. Krüppel-like factor 4 synergizes with CREB to increase the activity of apolipoprotein E gene promoter in macrophages. *Biochem Biophys Res Commun* 2015; **468**:66−72.
69. Luan B, Yoon YS, Le Lay J, Kaestner KH, Hedrick S, Montminy M. CREB pathway links PGE2 signaling with macrophage polarization. *Proc Natl Acad Sci USA* 2015;**112**:15642−7.
70. Liao X, Sharma N, Kapadia F, Zhou G, Lu Y, Hong H, et al. Krüppel-like factor 4 regulates macrophage polarization. *J Clin Investig* 2011; **121**:2736−49.
71. Chen S, Saeed AFUH, Liu Q, Jiang Q, Xu H, Xiao GG, et al. Macrophages in immunoregulation and therapeutics. *Signal Transduct Targeted Ther* 2023;**8**:207.
72. Abdelaziz MH, Abdelwahab SF, Wan J, Cai W, Huixuan W, Jianjun C, et al. Alternatively activated macrophages; a double-edged sword in allergic asthma. *J Transl Med* 2020;**18**:58.
73. Wang J, Liu Y, Ding H, Shi X, Ren H. Mesenchymal stem cell-secreted prostaglandin E2 ameliorates acute liver failure *via* attenuation of cell death and regulation of macrophage polarization. *Stem Cell Res Ther* 2021;**12**:15.